ELSEVIER

Journal of Chromatography B, 699 (1997) 47–61

JOURNAL OF CHROMATOGRAPHY B

Review

Permeable packings and perfusion chromatography in protein separation

Alírio E. Rodrigues

Laboratory of Separation and Reaction Engineering, Faculty of Engineering, University of Porto, 4099 Porto Codex, Portugal

Abstract

The use of permeable packings in perfusion chromatography for protein separation is reviewed. Mass transport mechanisms in large-pore materials include forced convection in addition to diffusive transport. The key concept in perfusion chromatography is the "augmented" diffusivity by convection which explains the improved efficiency of perfusive packings compared with conventional supports. An extended Van Deemter equation has to be applied when calculating the height equivalent to a theoretical plate (HETP) of chromatographic columns with flow-through particles. It is shown that the effect of forced convective flow in pores is to drive the separation performance between diffusion-controlled and equilibrium limits. A methodology to understand mass transfer mechanisms in permeable packings is proposed. Experimental results for protein separation by high-performance liquid chromatography in new packing media are discussed. Simulated moving bed technology is addressed. © 1997 Elsevier Science B.V.

Keywords: Reviews; Proteins

Contents

0378-4347/97/$17.00
PII S0378-4347(97)00197-7

1. Introduction

The need for "large-pores" or throughpores (above 1000 Å) associated with diffusive (small) pores has long been recognized in the patent literature in relation with catalyst preparation for reaction engineering applications [1,2]. In permeable packings intraparticle forced convection is a mass transport mechanism which must be considered in addition to diffusive transport. Permeable materials containing "large-pores" are also used in chemical engineering as adsorbents, HPLC packings, membranes, building materials or supports for biomass growth and cell culture. Examples include polystyrene materials for HPLC like POROS (PerSeptive Biosystems, USA) with pores of 7000 Å in diameter. A review of materials and processes used in separation engineering applications is shown in Table 1.

There are several ways of eliminating or reducing intraparticle mass transfer resistance as illustrated in Fig. 1, namely: (i) coating a nonporous support with an active species: this is the case of pellicular packings which have the disadvantage of low capacity; (ii) reducing the particle size: this leads to a decrease of the diffusion time constant but at the expense of higher pressure drop in the column and (iii) increasing particle permeability by carefully providing large pores for transport connected to smaller diffusive pores: this is the situation in perfusion chromatography.

New packing materials for chromatographic separation of proteins have been developed in the last decade and can be classified in several groups [8]: (a) homogeneous cross-linked polysaccharides; (b) macroporous polymers based on synthetic polymers; (c) tentacular sorbents and (d) materials based on the concept of "soft gel in a rigid shell".

The first group include particles such as agarose which have good capacity. The second group of packing is used in "perfusion chromatography" [18,19] whose high speed is possible because of the augmented diffusivity by intraparticle convection. Chromatographic media as POROS Q/M have

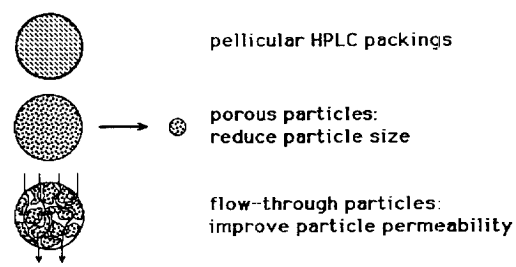

Fig. 1. Ways of reducing intraparticle mass transfer resistance.

Table 1
"Large-pore" materials for protein separation

Adsorbent Materials	Process	References
Alumina (Unisphere, Biotage, USA)	HPLC	[3]
Polystyrene (PL4000, Polymer Laboratories, UK)	HPLC	[4]
Polystyrene (POROS, PerSeptive Biosystems, USA)	HPLC	[5,6]
Silica gel (Daisogel SP 2705, Daiso)	HPLC	[7]
Hyper D (BioSepra, USA)	HPLC	[8,9]
TSK-PW (Toso-Haas, Japan)	HPLC	[10]
Fractogel (E. Merck, Germany)	HPLC	[11]
Silica (Nucleosil, Macherey-Nagel, Germany)	HPLC	[12]
Hydroxyapatite (HA Type S, Koken Bioscience Institute, Japan)	HPLC	[13]
Macro-Prep 50 (Bio-Rad Labs., USA)	Membrane chromatography	[14]
CM and DEAE MemSep (Millipore, USA)	Membrane chromatography	[15,16]
Pall (Dreieich, Germany)	Membrane chromatography	[17]

"throughpores" with a diameter of 6000–8000 Å and short diffusive pores of mean diameter 500–1000 Å. This combination allows proteins to enter more readily into the diffusive pores. "Perfusion chromatography" allows better column efficiency and higher separation speed than with conventional packings. The materials in group (c) are designed in such way that interaction between proteins to be separated and interactive groups is faster. Finally, materials in group (d) are developed in order to combine good sorption capacity of soft gels and rigidity of composite materials. Materials in this group are marketed under the name of Hyper D media (BioSepra, Villeneuve la Garenne, France).

The objectives of this review paper are: (i) to address mass transport mechanisms in permeable packings leading to the concept of "augmented" diffusivity by convection and show how it explains the improved performance of perfusion chromatography; (ii) to suggest a methodology for experimental studies on protein separations aiming at the characterization of chromatographic media and (iii) to describe simulated moving bed technology for bioseparations.

2. The concept of "augmented" diffusivity by convection

The use of permeable or flow-through particles has been increasing recently in relation with proteins separation by high-performance liquid chromatography (HPLC). The effect of intraparticle forced convective flow (viscous flow or Poiseuille flow) due to a total pressure gradient was noticed when measuring effective diffusivities by chromatographic techniques. The analysis of experimental results was first made with the conventional model which includes diffusion inside pores (in fact an "apparent" diffusivity $\tilde{D}_e$ lumping the "true" diffusivity D_e and convection). The "apparent" effective diffusivity $\tilde{D}_e$ was found to increase with the flow-rate. The enhancement of diffusivity by convection was named "augmented" diffusivity as explained by Rodrigues et al. [20]. For unretained species a simple relation between the "apparent" effective diffusivity, the "true" effective diffusivity and the intraparticle mass Peclet number was presented.

The key concept behind the improved performance of flow-through packings (gigaporous in Horvath's nomenclature, [21]) in adsorptive processes for protein separation [5,6], e.g., HPLC is that of intraparticle diffusivity augmented by convection inside transport pores [20]. In fact, the "augmented" diffusivity $\tilde{D}_e$ is related to the effective diffusivity D_e by:

$$\tilde{D}_e = D_e \frac{1}{f(\lambda)} \quad (1)$$

where $f(\lambda) = \frac{3}{\lambda}\left(\frac{1}{\tanh\lambda} - \frac{1}{\lambda}\right)$.

The key parameter is the intraparticle Peclet number λ defined as the ratio between the time constant for pore diffusion τ_d and the time constant for intraparticle convection τ_c, i.e., $\lambda = v_0 l / D_e$ where l is the characteristic dimension of the adsorbent particle and v_0 is the intraparticle convective velocity inside large-pores. Eq. (1) was derived on the basis of model equivalence between a complete model including mass transport inside pores by diffusion (D_e) and convection and a simpler model which lumped diffusion and convection in an "apparent" or "augmented" diffusivity $\tilde{D}_e$. The enhancement of diffusivity by intraparticle convection $1/f(\lambda) = \tilde{D}_e / D_e$ as a function of λ is shown in Fig. 2. There are two limiting situations: (i) diffusion-controlled case – at low bed superficial velocities u_0, the intraparticle convective velocity v_0 is also small; therefore $f(\lambda) = 1$ and so $\tilde{D}_e = D_e$; (ii) convection-controlled case – at high superficial velocities u_0, and therefore high v_0 and high λ, we get $f(\lambda) = 3/\lambda$; the augmented

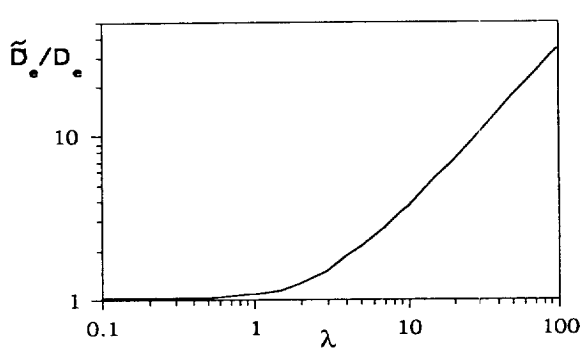

Fig. 2. Enhancement factor $\tilde{D}_e / D_e$ as a function of intraparticle Peclet number λ.

diffusivity is then $\tilde{D}_e = D_e\lambda/3 = v_0 l/3$ which depends only on the particle permeability, fluid viscosity and pressure drop across the particle. For spherical particles $l = R_p/3$ where R_p is the radius of the sphere in the calculation of the intraparticle Peclet number λ [3,22].

3. Perfusion chromatography

In the following section we will discuss the application of the key concept of "augmented" diffusivity by convection in perfusion chromatography of proteins.

3.1. Elution chromatography: the extended Van Deemter equation

The Van Deemter equation [23] for species linearly adsorbed in conventional packings of sphere geometry can be written as:

$$\text{HETP} = A + \frac{B}{u_0} + \frac{2}{15}\frac{\epsilon_p(1-\epsilon_b)b^2}{[\epsilon_b + \epsilon_p(1-\epsilon_b)b]^2}\tau_d u_0 \qquad (2)$$

where ϵ_p is the intraparticle porosity, ϵ_b is the bed porosity, $b = 1 + \{(1-\epsilon_p)/\epsilon_p\}m$ is the adsorption equilibrium parameter for a linear isotherm with slope m, and the time constant for diffusion is $\tau_d = \epsilon_p R_p^2/D_e$. In a condensed form, the Van Deemter equation is:

$$\text{HETP} = A + B/u_0 + Cu_0 \qquad (3)$$

where terms A, B and $C = \frac{2}{15}\frac{\epsilon_p(1-\epsilon_b)b^2}{[\epsilon_b + \epsilon_p(1-\epsilon_b)b]^2}\tau_d$ account for the contribution of eddy dispersion, molecular diffusion and intraparticle mass transfer to the HETP. The A term has been written in a semi-empirical form as proportional to u_0^n with $n = 0.33$ [24]. The velocity dependence of the A term is explained by some authors as a result of flow profiles in the bed; however, at high velocities the A term becomes constant.

For large-pore packings since $\tilde{D}_e = D_e/f(\lambda)$ or $\tilde{\tau}_d = \tau_d f(\lambda)$ the extended Van Deemter equation [25,26] is:

$$\text{HETP} = A + \frac{B}{u_0} + Cf(\lambda)u_0 \quad \text{(Rodrigues equation)} \qquad (4)$$

The Van Deemter equation for conventional supports (dashed line) and Rodrigues equation for large-pore supports (full line) are shown in Fig. 3 for a typical HPLC process. At low velocities $f(\lambda) \approx 1$ and both equations lead to similar results. However, at high superficial velocities, $f(\lambda) \approx 3/\lambda$, and therefore the last term in Rodrigues equation becomes a constant since the intraparticle convective velocity v_0 is proportional to the superficial velocity u_0. The HETP reaches a plateau which does not depend on the value of solute diffusivity but only on particle permeability and pressure gradient (convection-controlled limit). Permeable packings allow improved column performance since HETP is reduced when compared with conventional packings (the C term in Van Deemter equation is reduced). Moreover, the speed of separation can be increased (by increasing the superficial velocity) without losing column efficiency. Experimental results similar to the full line in Fig. 3 have been reported in HPLC of proteins [27–29] and in size-exclusion chromatography (SEC) [10,30].

The theoretical framework reviewed above allows complete calculations for linear perfusion chromatography. Protein separation by HPLC using large-pore packings is an area where the effect of intraparticle convective flow (of the order of 1% of the total flow through the bed) is sufficiently important to enhance the low diffusion coefficient for proteins

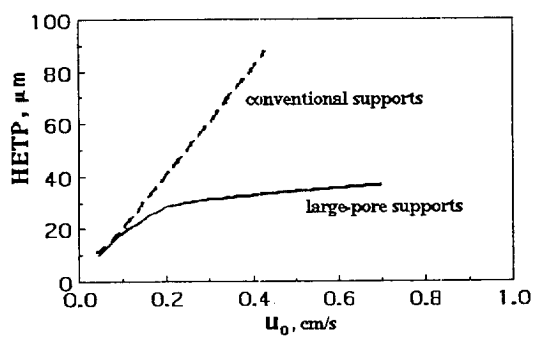

Fig. 3. HETP versus u_0 (Van Deemter equation for conventional packings and Rodrigues equation for large-pore packings).

($\approx 5\cdot 10^{-7}$ cm^2/s); therefore, intraparticle Peclet numbers λ of the order of 30 are easily obtained. However, if the kinetics of adsorption/desorption at the active sites of the packing is given by $\partial q_i'/\partial t = k_a c_i' - k_d q_i'$ (where c_i' and q_i' are the species concentrations in the fluid phase inside pores and in adsorbed phase, respectively and k_a and k_d are the kinetic constants for adsorption and desorption) the extended Van Deemter equation accounting for axial dispersion, film mass transfer, intraparticle diffusion, intraparticle convection and kinetics of adsorption/desorption at the fluid/solid interface becomes [31]:

$$\mathrm{HETP} = A + \frac{B}{u_0} + C\tau_d\left\{f(\lambda) + \frac{5}{\mathrm{Bi}_m} + \frac{3(b-1)}{b^2\phi_d^2}\right\}u_0 \quad (5)$$

Parameters accounting for film mass transfer are the Biot number $\mathrm{Bi}_m = k_f R_p/D_e$ and the Thiele modulus ϕ_d based on the desorption kinetic constant with $\phi_d^2 = \tau_d k_d$. Fig. 4 shows the effect of adsorption/desorption kinetics (ϕ_d) on the HETP versus u_0 plot. The performance of permeable packings is still better than that of conventional materials. In the extreme case of very slow adsorption/desorption kinetics the performances of both types of packings are very poor. One has to stress that intraparticle convection just enhances pore diffusivity but has no effect on the mechanism of adsorption/desorption. The extension of the Van Deemter equation to the case of bidisperse adsorbents containing macropores and micropores has been made by Carta and Rodrigues [22].

3.2. Frontal and displacement chromatography

In frontal chromatography a feed of constant concentration is passed through the column; at the outlet, the concentration as a function of time or eluted volume is the breakthrough curve. From the equilibrium theory of chromatography it is well known that compressive fronts are obtained in the case of favorable (Langmuir type) adsorption equilibrium isotherms. Moreover, in the presence of dispersive effects (axial dispersion, intraparticle mass transfer) the concentration wave will keep the shape as it moves through the bed (constant-pattern); the velocity of the concentration wave is equal to the shock velocity $u_{sh} = u_0/[\epsilon_b + (1-\epsilon_b)(\Delta q_i/\Delta c_i)]$ and depends on the slope of the chord connecting points representing the "feed state" and the "bed initial state".

For a binary mixture of proteins with favorable isotherms the less adsorbable protein will leave the bed in first place and can will reach a plateau at concentration higher than the feed. This is the "roll-up" phenomenon. Fig. 5 shows a sketch of the outlet concentration as a function of time for a binary mixture; the solution of the equilibrium model with axial dispersion is the full line and the solution of a pore-diffusion model is the dashed line. The effect of intraparticle convection is to drive the solution from

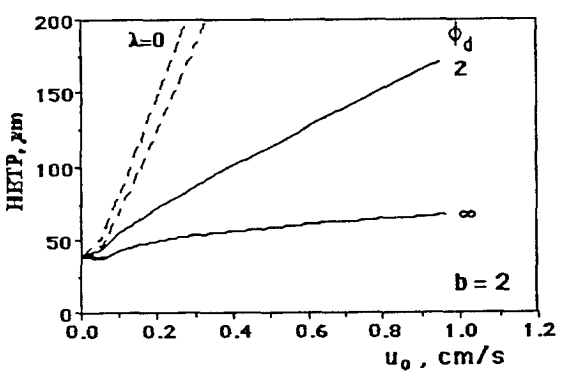

Fig. 4. Effect of adsorption/desorption kinetics on HETP vs. u_0 curves (dashed lines: conventional supports; full lines: permeable packings).

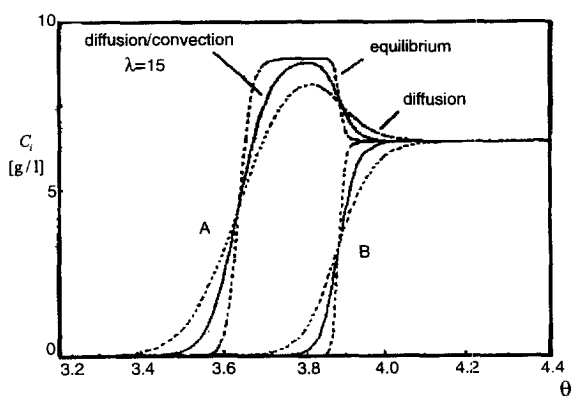

Fig. 5. Effect of intraparticle convection on the breakthrough curves of a binary mixture.

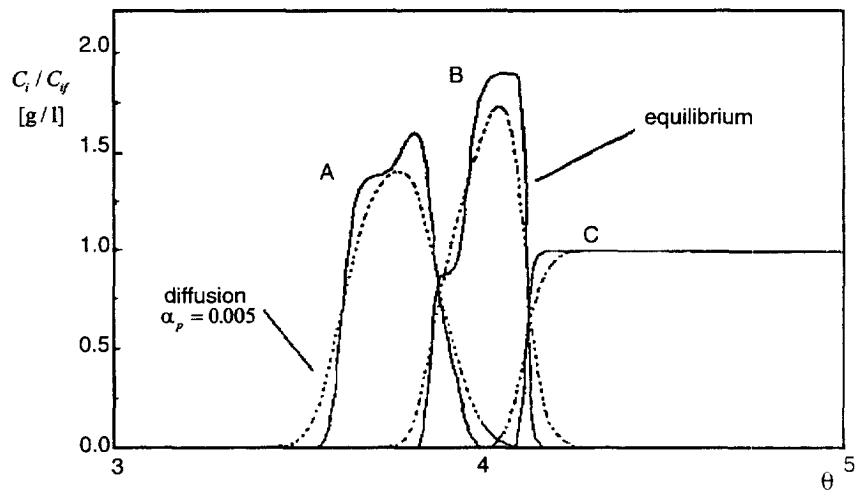

Fig. 6. Displacement chromatography of a binary mixture A/B with displacer C.

the diffusion case to the equilibrium case as shown with the dotted line.

Displacement chromatography is a powerful preparative technique for the separation of proteins. Feed species are bound to the column and then a displacer with higher affinity is passed through the column, creating a region of high concentration feed components adjacent to the displacer front. Fig. 6 compares chromatograms when a displacer C was used to separate a mixture of A and B; the solutions of the equilibrium + axial dispersion model (full line) and pore-diffusion model (dashed line) are shown.

4. Protein separations

4.1. Methodology for experimental studies

In this section the methodology for experimental studies in protein separations by HPLC using permeable packings will be discussed and examples presented. In order to understand the mass transfer mechanisms inside pores we suggest the following methodology: (i) elution chromatography experiments of proteins under unretained conditions – from these experiments HETP can be calculated as a function of flow-rate indicating which mass transport mechanisms are involved without extra effects of adsorption equilibrium; (ii) measurement of adsorption equilibrium isotherms by batch equilibration or from dynamic experiments using frontal chromatography leading to basic information on adsorbent capacity; (iii) measurement of breakthrough curves from which dynamic capacity of the adsorbent is calculated and (iv) modeling/simulation of HPLC columns and model validation.

4.2. Elution chromatography of proteins

In this section elution chromatography experiments under unretained conditions are performed to allow the understanding of mass transport mechanisms inside particles in the absence of extra effects related with protein adsorption. Studies are carried out in two anionic columns: (a) POROS Q/M (Prot. No. PO11M526, Serial No. 030, Packing Batch No. 033) purchased from PerSeptive Biosystems (Cambridge MA, USA). The dimensions of the POROS column were 100×4.6 mm I.D. with a bed volume of 1.7 ml packed with 20 μm diameter particles; (b) Q Hyper D cat No. 200227 Serial No. 32232 (UN 2196) from BioSepra, (Villeneuve la Garenne, France) with dimensions 100×5 mm I.D. packed with 35 μm diameter particles.

Three proteins were used: myoglobin (horse skeletal muscle, 95–100% purity), ovalbumin (albumin, chicken egg, 99% purity) and bovine serum albumin (BSA) (fraction V, 98–99% purity) were purchased from Sigma (St. Louis, MO, USA). The solvent used was 50 m*M* Tris–HCl, pH 8.6, mixed

with 0.5 *M* NaCl in HETP experiments. Temperature in all runs was 22°C.

The chromatographic experiments were carried on a Gilson 715 HPLC system equipped with a Model 360 pump, a manual injector (with an injection loop of 20 μl) and a Model 17UV ($\lambda = 280$ nm) detector. A computer system Gilson 715 HPLC software for data acquisition and a control system was used. Experiments with each protein were carried out at different flow-rates up to 10 ml/min corresponding to superficial velocities up to 1 cm/s.

The diffusivities of myoglobin, ovalbumin and BSA in aqueous solution at 25°C are respectively $16.1 \cdot 10^{-7}$, $6.4 \cdot 10^{-7}$ and $1 \cdot 10^{-7}$ cm^2/s [32].

4.2.1. Bed permeability

Bed permeabilities B_b were obtained from the slope of the plot $\Delta P/L$ versus the superficial velocity u_0. In laminar flow, the pressure drop ΔP across a bed of length L packed with particle d_p is given by Darcy's law $(\Delta P/L) = (\eta u_0/B_b)$ where $B_b = (\epsilon_b^3 d_p^2)/[150(1-\epsilon_b)^2]$ and ϵ_b is the bed porosity.

For the POROS column (20 μm particles) the bed permeability is $B_b = 2.35 \cdot 10^{-9}$ cm^2/s and $\epsilon_b = 0.34$; for the Hyper D column (35 μm particles) the bed permeability is $B_b = 1.02 \cdot 10^{-8}$ cm^2 and $\epsilon_b = 0.37$.

4.2.2. Estimation of intraparticle convective velocity v_0

The convective velocity v_0 in pores is estimated from the equality of pressure drops across the particle $\Delta p/d_p$ and across the bed $\Delta P/L$ [20,33]. In HPLC operation flow around the particles is in the laminar region ($Re < 0.1$) and the same applies for the convective flow inside pores. If B_b and B_p are bed and particle permeability, respectively, and η is the liquid viscosity, we get:

$$\frac{\Delta P}{L} = \frac{\eta}{B_b} u_0 \text{ and } \frac{\Delta p}{d_p} = \frac{\eta}{B_p} v_0 \tag{6}$$

and so:

$$v_0 = \frac{B_p}{B_b} u_0 \tag{7}$$

The fraction of flow-rate entering the column which goes through the macropores by convection is $(1-\epsilon)(B_p/B_b)$. For the Hyper D column (10 cm×5 mm) with 35 μm particles at a flow-rate of 8 ml/min or superficial velocity of 0.68 cm/s the bed pressure drop is $\Delta P = 7$ bar and so the pressure drop across the particle is $\Delta p = 245$ Pa.

4.2.3. Efficiency of chromatographic columns and HETP

Chromatographic peaks for the three proteins (BSA, myoglobin and ovalbumin) were obtained at various flow-rates on POROS Q/M and Q Hyper D supports. The HETP as a function of superficial velocity has been calculated for each protein from the experimental peaks in elution chromatography by $\text{HETP} = \sigma^2 L/\mu_1^2$ where σ^2 is the peak variance, μ_1 is the first moment of the peak and L is the column length.

Fig. 7 shows the experimentally measured reduced height equivalent to a theoretical plate ($h = \text{HETP}/d_p$) as a function of the bed superficial velocity u_0. It can be seen that for the POROS column, the HETP increases linearly at low superficial velocity and then, at high superficial velocities, reaches a plateau; and for the HYPER D column the HETP is almost a plateau, even at low u_0.

The efficiency of chromatographic columns can be easily characterized by its height equivalent to a theoretical plate (HETP); for columns packed with permeable packings Eq. (4) applies. The A term accounts for eddy dispersion effects and becomes a constant at high superficial velocities, $A = 2d_p$; $B = 2D_m$ and so the term B/u_0 can be neglected in the case of protein separation (at velocity $u_0 = 1$ cm/s, B/u_0 is around 10^{-7} cm). Film mass transfer resistance can also be neglected; film mass transfer coefficients estimated by available correlations [34] developed for purely diffusive media are conservative; in fact, in perfusive materials, intraparticle convection enhances film mass transfer [35]. The simplified equation for HETP is:

$$\text{HETP} \cong A + Cf(\lambda)u_0 \tag{8}$$

In the low velocity region where pore diffusion is the controlling mechanism of mass transfer, the slope of HETP versus u_0 is:

$$C = \frac{dH}{du_0} = \frac{1}{30} \frac{\nu}{(1+\nu)^2} \frac{\epsilon_p}{\epsilon_b} \frac{d_p^2}{D_e} \tag{9}$$

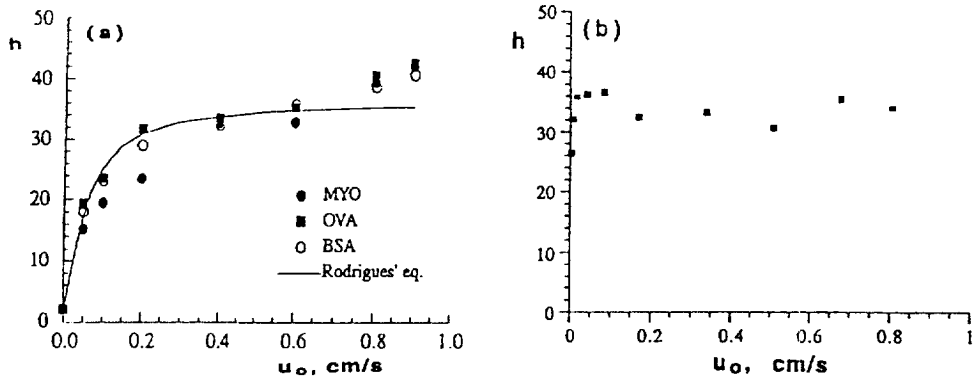

Fig. 7. HETP versus superficial velocity for elution chromatography of proteins under unretained conditions: (a) POROS Q/M; (b) Q HYPER D.

At high flow-rates $f(\lambda) \approx 3/\lambda$ and since $v_0 \propto u_0$ we get:

$$H_{\text{plateau}} = A + \frac{3}{5}\frac{\nu}{(1+\nu)^2}\frac{\epsilon_p}{\epsilon_b}\frac{B_b}{B_p}d_p \qquad (10)$$

where ν is $[(1-\epsilon_b)\epsilon_p]/\epsilon_b$. When the particle structure (ϵ_p) is known Eqs. (9) and (10) provide measured values of D_e and B_p. The straight line at low flow-rates crosses the plateau at a critical point $A + Cu_{0,c} = H_{\text{plateau}}$ and then $u_{0c} = (18D_e/d_p)(B_b/B_p)$. For POROS Q/M with $\epsilon_p = 0.5$ [19] we get $B_p = 1.5 \cdot 10^{-11}$ cm^2 for an experimental "h plateau" of 36 (reduced HETP) and $D_e = 7 \cdot 10^{-8}$ cm^2/s; for the Q HYPER D particles, the particle permeability was calculated from breakthrough experiments [36] as $B_p = 8.9 \cdot 10^{-12}$ cm^2 and a particle porosity of $\epsilon_p = 0.13$ is estimated from the plateau. The effective diffusivity calculated from modeling of breakthrough curves is $D_e = 8.1 \cdot 10^{-9}$ cm^2/s. The experimental HETP versus u_0 plot is almost a plateau indicating that gel diffusion should be the controlling factor at very low velocity and then paths are opened to allow intraparticle convection [37]. This is supported by results under weakly retained conditions described below.

4.2.4. Elution chromatography of proteins under weakly retained conditions

Elution experiments using BSA in a solution containing 0.3 *M* NaCl were carried out; from the peaks HETP was calculated as a function of the superficial velocity. Results obtained in our laboratory are shown in Fig. 8. The theoretical line according Rodrigues equation reasonably fits the experimental results using the values of effective diffusivity and particle permeability reported above. Clearly, the tendency towards a plateau on HETP would not be observed if intraparticle convection was not present. In this calculation linear adsorption equilibrium is taken into account.

4.3. Frontal chromatography experiments: measurement of adsorption equilibrium isotherms and breakthrough curves

In frontal chromatography experiments a solution of protein with concentration c_0 is continuously passed through the column under retained conditions (no salt in the feed). The concentration at the bed outlet as a function of time is the breakthrough curve

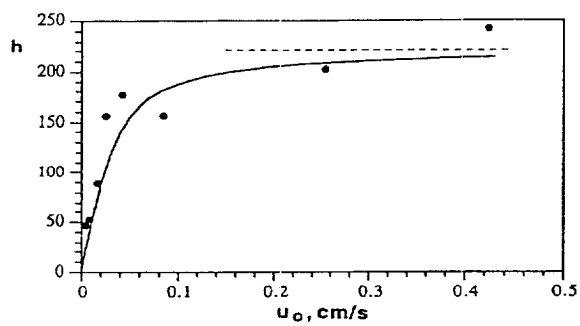

Fig. 8. HETP versus superficial velocity for elution chromatography of BSA on Q HYPER D under weakly retained conditions.

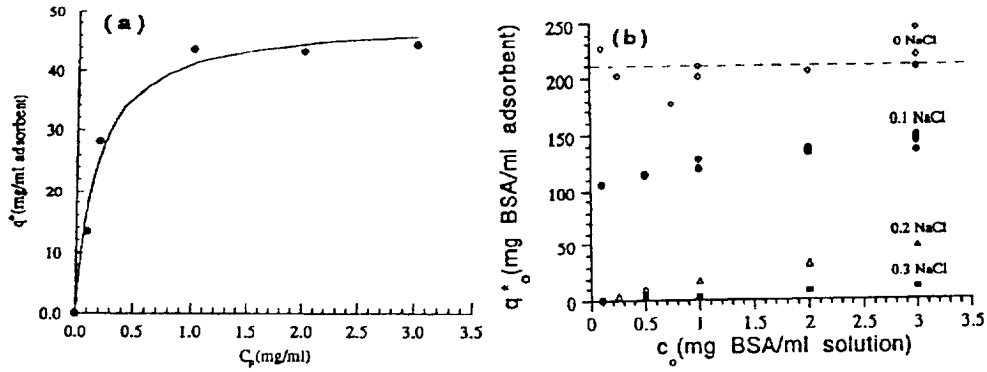

Fig. 9. Adsorption equilibrium isotherms of BSA on POROS Q/M (a) and Q HYPER D (b).

from which the amount of protein retained in the adsorbent q_0^* is calculated by mass balance. Therefore a point of the adsorption equilibrium isotherm can be calculated from one experiment with a given feed concentration c_0. The adsorption equilibrium isotherm of BSA in POROS Q/M shown in Fig. 9a follows Langmuir equation [29]. Adsorption equilibrium isotherms of BSA on Q HYPER D, at various salt concentrations, are shown in Fig. 9b. With no salt the isotherm is almost rectangular. With 0.3 *M* NaCl the protein is weakly retained with linear isotherm.

5. Simulated moving bed technology

5.1. What is SMB technology?

The simulated moving bed (SMB) technology developed by UOP [38] has been used in chemical industry for several separations known as SORBEX processes [39–42]. They include the Parex process for the recovery of *p*-xylene from a mixture of C_8 aromatics, the Molex process for the extraction of *n*-paraffins from branched and cyclic hydrocarbons, the Olex process to separate olefins from paraffins and the Sarex process for the recovery of fructose from fructose/glucose mixtures in the production of high frutose corn syrup HFCS [43–45]. More than hundred SMB units are operated worldwide [46]. The heart of the SMB technology is a rotary valve which periodically changes the position of feed, eluent, extract and raffinate lines along the bed. In this way the solid movement in a true moving bed (TMB) is simulated. Continuous chromatography in SMB also eliminates drawbacks of batch chromatography, namely dilution of species and low adsorbent utilization [47–51].

The SMB technology has been applied in the areas of biotechnology, pharmaceuticals and fine chemistry. Pilot and industrial SMB for such applications have been developed by UOP [52,53] and SEPAREX [54]. More recent applications are related with chiral technology [55,56]. It should be pointed out that scaling down of the Sorbex flowsheet becomes less economical than using a system of individual beds segmented by valves and feed and product lines [57].

5.2. Strategies of modeling

Models available in literature for SMB separation processes have been summarized by Ruthven and Ching [58]. The simulated moving bed can be represented by two different models: the real SMB and the true moving bed, TMB. In the SMB sketched in Fig. 10 the counter-current flow of the solid is simulated by moving the eluent, extract, feed and raffinate lines one column forward in the fluid flow direction at fixed time intervals. In the Sorbex technology this is achieved with a rotary valve; in the Licosep 12-26 there are 12 individual beds with valves in each column and corresponding lines for the various streams. The Licosep technology is a result of joint efforts of IFP (French Institute of Petroleum) and Separex [49]; the technology is now

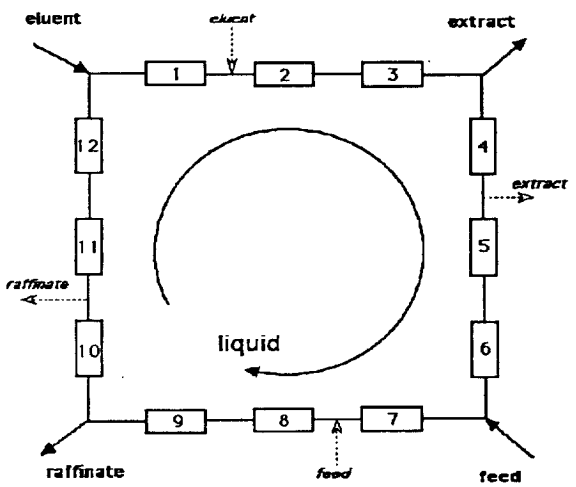

Fig. 10. Schematic diagram of the four-section SMB.

available through Novasep (Vandoeuvre-lès-Nancy, France).

In the true moving bed (TMB) shown in Fig. 11 the liquid and the solid phases flow in opposite directions. The liquid flowing out of zone IV is recycled to zone I while the solid coming out of zone I is recycled to zone IV. In both approaches zone I is located between eluent and extract nodes, zone II is between extract and feed nodes, zone III separates

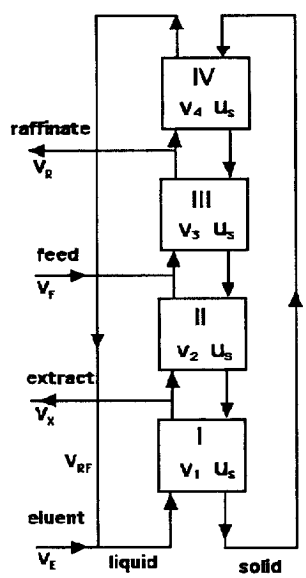

Fig. 11. Schematic diagram of the four-section TMB.

feed and raffinate nodes and finally zone IV is between raffinate and eluent nodes. Also, the less retained species A is recovered in the raffinate stream and the more retained species B is collected in the extract stream.

Both SMB and TMB systems have similar cyclic steady-state performances; therefore, one can simulate and obtain the optimum operating conditions for the SMB, using the TMB model since it requires lower computing time. In fact, the cyclic behaviour of the simulated moving bed can be calculated from the steady-state model of the true moving bed, taking into account the relation between the solid velocity u_s and the rotation period (or switching time) ΔT in SMB operation, i.e., $u_s = L/\Delta T$, where L is the column length.

The equivalence between the SMB and its corresponding TMB is made by keeping constant the liquid velocity relative to the solid velocity, i.e., $v_j^{SMB} = v_j^{TMB} + u_s$, where v_j is the interstitial fluid velocity in the j section of the moving bed.

5.2.1. A package for SMB simulation

The package developed for the transient TMB system considers axial dispersion flow for the bulk fluid phase, linear driving force (LDF) for the intraparticle mass transfer rate and takes into account multicomponent adsorption equilibria. The model equations in dimensionless form [59,60] are:

Mass balance:

$$\frac{1}{\mathrm{Pe}}\frac{\partial^2 c_{ij}}{\partial x^2} - \frac{\partial c_{ij}}{\partial x} + \frac{1-\epsilon_b}{\epsilon_b}\frac{1}{\gamma_j}\frac{\partial q_{ij}}{\partial x} = \frac{1}{\gamma_j}\frac{\partial c_{ij}}{\partial \theta} + \frac{1-\epsilon_b}{\epsilon_b}\frac{1}{\gamma_j}\frac{\partial q_{ij}}{\partial \theta} \tag{11}$$

Intraparticle mass transfer rate:

$$\frac{\partial q_{ij}}{\partial x} + \alpha_j(q_{ij}^* - q_{ij}) = \frac{\partial q_{ij}}{\partial \theta} \tag{12}$$

Boundary conditions:

$$x = 0 \quad c_{ij} - \frac{1}{\mathrm{Pe}_j}\frac{\mathrm{d}c_{ij}}{\mathrm{d}x} = c_{ij,0} \tag{13a}$$

$$x = 1 \quad \frac{\mathrm{d}c_{ij}}{\mathrm{d}x} = 0 \text{ and } q_{ij} = q_{ij+1,0} \tag{13b}$$

Multicomponent adsorption equilibrium isotherm:

$$q_{Aj}^{*} = f_A(C_{Aj}, C_{Bj})$$
$$q_{Bj}^{*} = f_B(C_{Aj}, C_{Bj}) \quad (14)$$

Mass balances at the nodes of the inlet and outlet lines of the TMB:

Eluent node: $$c_{i1,0} = \frac{\nu_4}{\nu_1} c_{i4,L_j} \quad (15a)$$

Extract node: $$c_{i2,0} = c_{i1L_j} \quad (15b)$$

Feed node: $$c_{i3,0} = \frac{\nu_2}{\nu_3} c_{i2,L_j} + \frac{\nu_F}{\nu_3} c_i^F \quad (15c)$$

Raffinate node: $$c_{i4,0} = c_{i3L_j} \quad (15d)$$

with the relations between fluid velocities in the four zones of TMB: $\nu_4 = \nu_{RF}$, $\nu_1 = \nu_4 + \nu_E$, $\nu_2 = \nu_1 - \nu_x$, $\nu_3 = \nu_2 + \nu_F$. In the above model equations i (i=A,B) refers to the species in the mixture and j (j=1,2,3,4) is the section number, c_{ij} and q_{ij} are the fluid phase and average adsorbed phase concentrations of species i in section j of the TMB, respectively, $x = z/L_j$ is the dimensionless axial coordinate, $\theta = t/\tau_s$ is the dimensionless time variable, with $\tau_s = L_j/u_s = N_s\Delta T$ (N_s is the number of columns per section; u_s is the solid velocity), v_j is the fluid velocity and q_{ij}^{*} is the adsorbed phase concentration in equilibrium with c_{ij}. Model parameters are: $(1-\epsilon_b)/\epsilon_b$ (ratio between solid and fluid volumes), $\gamma_j = v_j/u_s$ (ratio between fluid and solid velocities), $Pe_j = v_j L_j/DL_j$ (Peclet number; D_{Lj} is the axial dispersion coefficient in section j) and $\alpha_j = kL_j/u_s = k\tau_s$ (number of intraparticle mass transfer units; k is the intraparticle mass transfer coefficient). Adsorption equilibrium parameters have to be added to the list above.

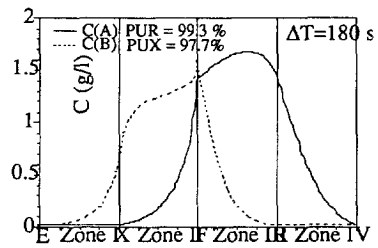

Fig. 12. Internal profiles for the reference case.

5.2.2. Effect of rotation period and number of intraparticle mass transfer units on performance parameters

The SMB performance is characterized by four process parameters: purity, recovery, solvent consumption and adsorbent productivity. For the case of a binary separation in the SMB in which the less retained species A is recovered in the raffinate, and the more retained component B is recovered in the extract, process performance parameters are defined in Table 2.

The effects of the rotation period and number of intra-particle mass transfer units on the SMB performance were studied by simulation. A reference case relative to a 8-column configuration of the SMB was chosen and the influence of several operating variables was studied by simulation. The internal profiles for such case are shown in Fig. 12.

5.2.2.1. *Effect of the rotation period.* The influence of the rotation period on the system performance is shown in Fig. 13. It can be seen that high purities and recoveries can be obtained only in a narrow window of rotation periods. A similar behaviour could be obtained by changing the value of the liquid

Table 2
Performance criteria for SMB

Performance parameter	Extract X	Raffinate R
Purity (%)	$100C_X^B/(C_X^A + C_X^B)$	$100C_R^A/(C_R^A + C_R^B)$
Recovery (%)	$100C_X^B Q_X/(C_F^B Q_F)$	$100C_R^A Q_R/(C_F^A Q_F)$
Solvent consumption (l/g)	$(Q_E + Q_F)/C_X^B Q_X)$	$(Q_E + Q_F)/(C_R^A Q_R)$
Productivity (g/h l of solid)	$C_X^B Q_X/V_S$	$C_R^A Q_R/V_S$

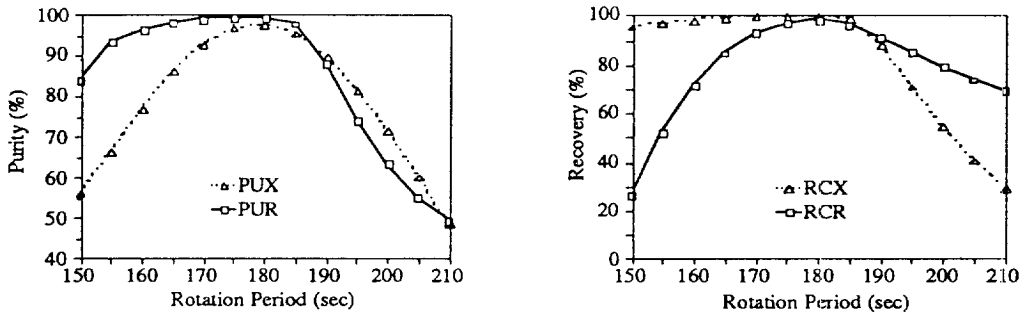

Fig. 13. Effect of the rotation period on purity and recovery.

recycling flow-rate instead of the rotation period; in fact, the rotation period or switching time is inversely proportional to the solid flow-rate so the role of increasing the recycling liquid flow-rate or decreasing the solid flow-rate (increasing ΔT) is similar with regard to the calculation of the net flux of a species.

5.2.2.2. *Effect of the number of intraparticle mass transfer units.* The effect of the intraparticle mass transfer rate k or the corresponding dimensionless number α on the cyclic steady-state internal profiles of the SMB is shown in Fig. 14 for $\alpha=36$ and $\alpha=180$ (or $k=0.1\ s^{-1}$ and $k=0.5\ s^{-1}$). The mass transfer coefficient depends only on the intraparticle diffusivity of species and particle size. Therefore, increasing α (or k) by decreasing the particle size improves the performance of the SMB, provided the constraint of acceptable pressure drop is met. Some applications in the area of protein processing will use large-pore permeable particles in which intraparticle mass transport by convective flow is important, leading to an enhancement of the mass transfer rate. The above model can still be used in that case if the mass transfer coefficient k is replaced by an "augmented" mass transfer coefficient $\tilde{k}$ [61].

6. Conclusions

In this review it is shown that the key concept behind the improved performance of large-pore, permeable packings used in perfusion chromatography is the "augmented " diffusivity by convection. This concept has long been recognized in the reaction engineering area and explains how perfusion chromatography works. An extended Van Deemter equation as derived by Rodrigues [25] allows the prediction of HETP as a function of superficial velocity in perfusion chromatography.

A methodology for studying protein adsorption in permeable packings is suggested. First, elution chro-

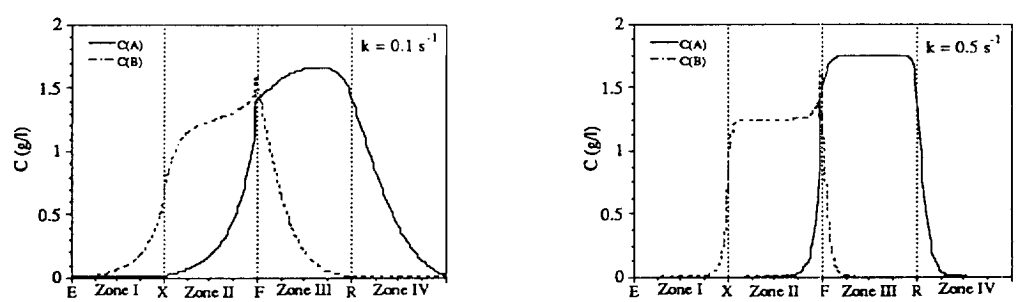

Fig. 14. Effect of the intraparticle mass transfer rate on the cyclic steady-state SMB internal profiles.

matography experiments should be carried out under unretained conditions to allow easy understanding of mass transport mechanisms inside permeable particles. This is to be complemented with particle characterization [62] and direct methods to measure convective flow inside flowthrough particles [63]. Secondly, experiments under weakly retained conditions in the linear region of adsorption equilibrium isotherm should be performed to check the influence of the adsorption parameter b. Frontal chromatography experiments allow the calculation of adsorption equilibrium isotherm and also information on the dynamic capacity of the bed. Finally, modeling and simulation [64–68] allow design of chromatographic columns under conditions different from those at laboratory scale [69–72].

Experiments with new chromatographic media show that intraparticle convection is an important mass transport mechanism in such materials. Elution chromatography experiments with POROS Q/M adsorbent show clearly the presence of a intraparticle convective flux that enhances the mass transport performance of large-pore chromatographic supports. The reduced HETP vs. superficial bed velocity plot, obtained for non-retained BSA, myoglobin and ovalbumin, allowed the calculation of a particle porosity $\epsilon_p = 0.5$ from the plateau and an approximate effective diffusivity $D_e = 7 \cdot 10^{-8}$ cm^2/s from the initial slope. On the other hand, experimental results with Q HYPER D particles indicate that at very low flow-rates gel diffusion is the controlling mechanism; as flow-rate increases, pore diffusion becomes the main mass transfer process and at higher flow-rates, the process is fully convection controlled. From the plateau of the reduced HETP a particle porosity $\epsilon_p = 0.13$ is obtained; from the slope an effective diffusivity of $D_e = 8.1 \cdot 10^{-9}$ cm^2/s is extracted.

SMB technology is now becoming used in the area of bioseparations. A model for predicting the cyclic steady-state behaviour of the simulated moving bed (SMB) is developed using the correspondent true moving bed (TMB) approach. The model also enables the prediction of the TMB transient behaviour. This SMB package is an important learning and training tool used to predict the effect of operating variables on the process performance, and so the choice of the best conditions for the SMB operation.

7. List of symbols

b	adsorption equilibrium parameter
Bi_m	mass Biot number, dimensionless
B_b	bed permeability, m^2
B_p	particle permeability, m^2
c_p	protein concentration in the pore fluid phase, mol/m^3
c_0	feed concentration of protein in the external fluid phase, mol/m^3
c	concentration in the fluid phase at the column outlet, mol/m^3
c_{ij}	fluid phase concentration of component i in section j, kg/m^3
d_p	particle diameter, m
D_e	effective diffusivity, m^2/s
$\tilde{D}_e$	augmented effective diffusivity, m^2/s
D_m	molecular diffusivity, m^2/s
D_{Lj}	axial dispersion coefficient in the j section, m^2/s
h	reduced HETP (HETP/d_p), dimensionless
H	height equivalent to a theoretical plate, m
HETP	height equivalent to a theoretical plate, m
k_f	film mass transfer constant, m/s
k	intraparticle mass transfer coefficient, s^{-1}
l	characteristic dimension of the particle, m
L	bed length, m
L_j	section length, m
M	solid flow-rate, m^3/s
N_s	number of columns per section in the SMB system
Pe_j	Peclet number for section j ($=v_j L_j / D_{Lj}$)
Δp	pressure drop across the particle, bar
ΔP	bed pressure drop, bar
q_{ij}	average adsorbed phase concentration of component i in section j, kg/m^3 adsorbent
q_{ij}^*	adsorbed concentration of component i in section j in equilibrium with C_{ij}, kg/m^3 adsorbent
q_0^*	adsorbed phase concentration in equilibrium with c_0, mg/ml adsorbent
R_p	particle radius, m
t	time variable, s
ΔT	rotation period, s
u_s	solid velocity, m/s
u_0	bed superficial velocity, m/s
$u_{0,c}$	critical velocity, m/s
v_0	intraparticle convective velocity, ms

v_j interstitial fluid velocity in the j section, m/s
V bed volume, m^3
V_s volume of the solid phase, m^3
x dimensionless axial coordinate ($=z/L_j$)
z axial coordinate in the column, m

7.1. Greek symbols

α_j number of mass transfer units ($=k\tau_s$), dimensionless
ϵ_b bed porosity (interparticle volume/bed volume)
ϵ_p intraparticle porosity (pore volume/particle volume)
λ intraparticle Peclet number
η fluid viscosity, g/cm. s
μ_1 1st order moment of the impulse response
ν $(1-\epsilon_b)\epsilon_p/\epsilon_b$
σ^2 variance
τ space time, cm
τ_c time constant for convection, s
τ_d time constant for diffusion, s
$\tilde{\tau}_d$ "apparent" time constant for diffusion, s
γ_j ratio between fluid and solid velocities ($=v_j/u_s$), dimensionless
θ dimensionless time, ($=t/\tau_s$)
τ_s solid space time, ($=L_j/u_s$), s

Acknowledgements

A.R. acknowledges the contribution of M. Rendueles de la Vega, C. Chenou and L. Pais for the experimental work on protein separation and SMB studies.

References

[1] A. Nielsen, S. Bergh and B. Troberg, US Pat. 3 243 386, Mar 29, 1966.
[2] N. Harbord, UK Pat. 1 484 864, Sept 8, 1977.
[3] G. Carta, H. Massaldi, M. Gregory, D. Kirwan, Sep. Technol. 2 (1992) 62.
[4] L. Lloyd, F. Warner, J. Chromatogr. 512 (1990) 365.
[5] N. Afeyan, F. Regnier and R. Dean, Jr., US Pat. No. 5 019 270, May 28, 1991.
[6] N. Afeyan, F. Regnier and R. Dean, Jr., US Pat. No. 5 228 989, July 20, 1993.
[7] Daisogel SP2705, Technical Literature, Daiso, Osaka, 1991.
[8] E. Boschetti, J. Chromatogr. A 658 (1994) 207.
[9] J. Horvath, E. Boschetti, L. Guerrier rier, N. Cooke, J. Chromatogr. A 679 (1994) 11.
[10] M. Potschka, J. Chromatogr. 648 (1993) 48.
[11] Fractogel Technical Literature, E. Merck, Germany, 1987.
[12] Nucleosil 4000-7PEI, Technical Literature, Macherey-Nagel, Germany, 1989.
[13] T.J. Kawasaki, J. Chromatogr. 544 (1991) 147.
[14] K. Talmadge, L. Dunn, M. Abouelezz, H. Morehead, M. Navvab, C. Ordunez, T. Tish, C. Siebert, J. Chromatogr. 590 (1992) 83.
[15] A. Shiosaki, M. Goto, T. Hirose, J. Chromatogr. A 679 (1994) 1.
[16] J. Gerstner, R. Hamilton, S. Cramer, J. Chromatogr. 596 (1992) 173.
[17] K.G. Briefs, M.R. Kula, Chem. Eng. Sci. 47 (1992) 141.
[18] N. Afeyan, S. Fulton, N. Gordon, I. Mazsaroff, L. Varady, F. Regnier, Biotechnology 8 (1990) 203.
[19] N. Afeyan, N. Gordon, I. Mazsaroff, L. Varady, S. Fulton, Y. Yang, F. Regnier, J. Chromatogr. 519 (1990) 1.
[20] A.E. Rodrigues, B. Ahn, A. Zoulalian, AIChEJ 28 (1982) 541.
[21] Cs. Horváth, Preparative HPLC, NATO ASI Chromatographic and Membrane Processes in Biotechnology, Azores, 1990.
[22] G. Carta, A.E. Rodrigues, Chem. Eng. Sci. 48 (1993) 3927.
[23] J. Van Deemter, F. Zuiderweg, A. Klinkenberg, Chem. Eng. Sci. 5 (1956) 271.
[24] J.H. Knox, Anal. Chem. 38 (1966) 253.
[25] A.E. Rodrigues, LC·GC 6 (1993) 20.
[26] A.E. Rodrigues, J. Lopes, M. Dias, J. Loureiro, Z. Lu, J. Chromatogr. 590 (1992) 93.
[27] N. Afeyan, S. Fulton, F. Regnier, J. Chromatogr. 544 (1991) 267.
[28] D. Frey, E. Schwesnheim, Cs. Horváth, Biotech. Prog. 9 (1993) 273.
[29] A.E. Rodrigues, C. Chenou, M. Rendueles de la Vega, Chem. Eng. J. 61 (1996) 191.
[30] M. Van Kreveld, N. Van den Hoed, J. Chromatogr. 149 (1978) 71.
[31] A.E. Rodrigues, A. Ramos, J. Loureiro, M. Dias, Z. Lu, Chem. Eng. Sci. 47 (1992) 4405.
[32] M. Tyn, T. Gusek, Biotechnol. Bioeng. 35 (1990) 327.
[33] H. Komiyama, H. Inoue, J. Chem. Eng. Japan 7 (1974) 281.
[34] T. Kataoka, H. Yoshida, K. Ueyama, J. Chem. Eng. Japan 5 (1972) 132.
[35] Z.P. Lu, D. Frey, A.E. Rodrigues, Ind. Eng. Chem. Res. 32 (1993) 2159.
[36] A.E. Rodrigues, in M. Potschka and P. Dubin (Editors), Strategies in Size-Exclusion Chromatography, 1996, ACS Symp. Series, Vol. 635, pp. 158–172.
[37] A.E. Rodrigues, J. Loureiro, C. Chenou, M. Rendueles de la Vega, J. Chromatogr. B 664 (1995) 233.
[38] D.B. Broughton, US Pat. 2 985 589, 1961.

[39] A.J. de Rosset, R.W. Neuzil and D.B. Broughton, in A.E. Rodrigues and D. Tondeur (Editors), Percolation Processes, Theory and Applications, Sijthoff and Noordhoff Publishers, Netherlands, 1981.
[40] J.A. Johnson, in A.E. Rodrigues, D. Tondeur and D. Levan (Editors), Adsorption: Science and Technology, Kluwer Academic Publishers, Netherlands, 1989.
[41] J.A. Johnson and R.G. Kabza, in G. Ganetsos and P.E. Barker (Editors), Preparative and Production Scale Chromatography, Marcel Dekker, New York, 1993.
[42] D.B. Broughton, Chem. Eng. Prog. 64 (1968) 60.
[43] D.B. Broughton, Chem. Eng. Prog. 66 (1970) 70.
[44] D.B. Broughton, Sep. Sci. Technol. 19 (1984) 723.
[45] J.L. Humphrey, Chem. Eng. Prog. 31-41 (1995) 31.
[46] M. Bailly, D. Tondeur, G. Grevillot, Informations Chimie 255 (1984) 237.
[47] B. Balannec and G. Hotier, in G. Ganetsos and P.E. Barker (Editors), Preparative and Production Scale Chromatography, Marcel Dekker, New York, 1993.
[48] G. Hotier, B. Balannec, Revue de l'Institut Français du Pétrole 46 (1991) 803.
[49] M. Bailly and R.M. Nicoud, in C. Rivat and J. Stoltz (Editors), Biotechnology of Blood Proteins, Colloque INSERM/John Libbey Eurotext, Vol. 227, 1993, p. 13.
[50] R.M. Nicoud, Simulated Moving Bed: Basics and Applications, European Meeting, Nancy, 1993.
[51] K. Gottschall, M. Kay and J. Reusch, Simulated Moving Bed Chromatography, PREP'94, Baden-Baden, Germany, 1994.
[52] M. Gattuso, B. McCulloch and J.W. Priegnitz, in Chiral Europe, 1994.
[53] M. Gattuso, B. McCulloch, D.W. House, and W.M. Baumann, in Chiral USA, 1995.
[54] R.M. Nicoud, LC·GC Int. 5 (1992) 43.
[55] R.A. Sheldon, Chirotechnology: Industrial Synthesis of Optically Active Compounds, Marcel Dekker, New York, 1993.
[56] S.C. Stinton, Chiral Drugs, C and EN, Vol. 44–74, Oct 1995.
[57] G.E. Keller, II, Chem. Eng. Prog. 102 (1995) 56.
[58] D. Ruthven, C.B. Ching, Chem. Eng. Sci. 44 (1989) 1011.
[59] A. Rodrigues, Z.P. Lu, J.M. Loureiro, L.S. Pais, J. Chromatogr. A 702 (1995) 223.
[60] L. Pais, J. Loureiro, A. Rodrigues, Chem. Eng. Sci. 52 (1997) 245.
[61] A. Leitão, A. Rodrigues, Chem. Eng. J. 60 (1995) 81.
[62] K.C. Loh, D.I.C. Wang, J. Chromatogr A. 718 (1995) 239.
[63] J. Pfeiffer, J. Chen, J.T. Hsu, AIChEJ 42 (1996) 932.
[64] A.E. Rodrigues, Z.P. Lu, J. Loureiro, Chem. Eng. Sci. 46 (1991) 2765.
[65] A.E. Rodrigues, Z. Lu, J. Loureiro, G. Carta, J. Chromatogr. A 653 (1993) 189.
[66] A.I. Liapis, M. McCoy, J. Chromatogr A. 660 (1994) 85.
[67] G. Heeter, A.I. Liapis, J. Chromatogr A. 734 (1996) 105.
[68] A.I. Liapis, Y. Xu, O. Crosser, A. Tongta, J. Chromatogr A. 702 (1996) 45.
[69] J. Gerstner, T. Londo, T. Hunt, J. Morris, P. Pedroso, R. Hamilton, Chemtech Nov (1995) 27.
[70] J.C. Janson and L. Ryden, Protein Purification, VCH Publishers, Weinheim, 1989.
[71] M. Ladisch, R. Willson, C. Painton and S. Builder (Editors), Protein Purification: From Molecular Mechanisms to Large-Scale Processes, ACS Symposium Series 427, 1990.
[72] J.C. Janson and P. Hedman, in A. Fiechter (Editor), Advances in Biochemical Engineering, Vol. 25, 1982, p. 43.